ADAPTIVE MATERIALS AND AEROSTRUCTURES: REVOLUTIONIZING AEROSPACE SYSTEMS

Ron Barrett*

Abstract

This paper describes some of the most unique and dynamic aerospace technologies of our time. A brief historical overview traces modern Adaptive Aerostructures to their roots in subsystems of the F-14, through the bending, twisting plates of the 1980's and the first warping-wing patents of the early 1990's. This paper includes an overall description of the latest adaptive actuation technologies using Post-Buckled Precompressed (PBP) actuators, which enabled the first morphing-wing UAVs and world's first post-stall maneuvering, convertible UAV which hovers like a helicopter then dashes like a missile. The paper describes the fundamental structural mechanics of these actuators and shows that they can provide up to an order of magnitude better performance than conventional adaptive actuators approaches. The paper describes future systems using such actuators in aircraft as small as 5mm to the nacelles of widebody aircraft. Coming advances are described including the latest and most capable flutter test and flight control surfaces for general aviation aircraft, business jets and commercial transports. The document concludes with a summary of the most modern optically adaptive materials and describes their performance in the first unclassified visual stealth aircraft.

Keywords: Adaptive Aerostructures, Piezoelectric, Flight Control, MAV, UAV, Missile, Munition, Widebody

Nomenclature

a	integrating factor, acceleration	~, g's
A	in-plane laminate stiffness	lb/in (N/m)
A_f	Austenitic finish transition temperature	C
A_s	Austenitic start transition temperature	C
AR	PBP Amplification Ratio = $\delta(F_a>0)/\ \delta(F_a=0)$	
b	actuator width	in (mm)
B	coupling laminate stiffness	lb (N)
c	integrating factor	
C_{h_α}	hinge moment coefficient with angle of attack	(deg^{-1})
C_{h_δ}	hinge moment coefficient with deflection	(deg^{-1})
C_l	section lift coefficient	
C_L	aircraft lift coefficient	
C_M	pitching moment coefficient	
D	bending laminate stiffness	in-lb (N-m)
E	stiffness	GPa (msi)
M	applied moment vector	N-m/m (in-lb/in)
M_f	Martensitic finish transition temperature	C
M_s	Martensitic start transition temperature	C
N	applied force vector	N/m (lb/in)
t	thickness	in (mm)
y	out of plane displacement dimension	in (mm)
z	through thickness dimension	in (mm)
α	angle of attack	deg
δ	PBP beam angle	deg
δ_o	PBP end rotation angle	deg
ε	laminate in-plain strain	µstrain
κ	laminate curvature	rad/in (rad/m)
Λ	piezoelectric free element strain	µstrain
σ	stress	msi (GPa)

Subscripts

a	actuator
b	bond
ex	external
ht	high temperature
l	laminate
lt	low temperature
s	substrate
t	thermally induced

Acronyms

BLAM	Barrel-Launched Adaptive Munition
DAP	Directionally Attached Piezoelectric
DEAS	Dynamic Elastic Axis Shifting
FCS	Flight Control Surface
FTS	Flutter Test Surface
LNPS	Low Net Passive Stiffness
MAV	Micro Aerial Vehicle
NAV	Nano Aerial Vehicle
Nitinol	Nickel-Titanium Shape Memory Alloy
PBP	Post-Buckled Precompressed
PZT	Lead Zirconate Titanate
SCRAM	Smart Compressed Reversed Adaptive Munition
SMA	Shape Memory Alloy
StAB	Steerable Adaptive Bullet
SST	Sky Shaker Technologies, LLC
TNO	Toegepast Natuurwetenschappelijk Onderzoek
TUD	Technical University of Delft, Netherlands
TTR	Temperature Transition Range
UAV	Uninhabited Aerial Vehicle
ZNPS	Zero Net Passive Stiffness

Professor and Director of the Adaptive Aerostructures Laboratory, Department of Aerospace Engineering, The University of Kansas, Lawrence, Kansas 66045 Email: adaptivebarrett@yahoo.com

Introduction and Background

For nearly 4 decades now, adaptive materials and structures have been regularly fielded with advanced aircraft, systems and aerospace subsystems. These materials have consistently improved the performance of aerospace vehicles by offering lower weight, tighter installation volumes, lower power consumption, higher energy density and overall cost savings over their conventional counterparts. These shape- and property-changing materials are being found on the latest incarnations aircraft ranging from tiny micro aerial vehicles (MAVs) and nano aerial vehicles (NAVs) to commercial transports with ever-more applications coming almost daily.

The roots of the field stretch back into the 1880's (considering piezoelectric actuators) and in the case of shape memory alloys (SMA's), the 1930's. Indeed, it was Jacques and Pierre Curie who discovered piezoelectric properties in Rochelle salts nearly 130 years ago. These unique salts had the unusual capability of converting mechanical strain energy into electrical energy and visa versa.[1-3] For this early work, Pierre Curie claimed the prestigious Plante Prize in Physics. For several decades, the field of piezoelectricity remained a relative scientific curiosity until it was discovered that X-cut quartz crystals could be used to generate pulses in water. By measuring the time between outgoing and incoming pulse, the distance to a given target could be measured, and so was born Sonar in the second decade of the 20th century.[2] From these humble beginnings, piezoelectric applications exploded following the discovery that stable radio transmitter and receivers could be structured around tuned piezoelectric crystals. Many dozens of patents were issued between the 1920's and '30's until by the start of WWII, piezoelectric crystal radio gear had become the standard, supplanting vacuum tube technology in tuners. So in the strictest sense, piezoelectric materials were the first class of man-made adaptive materials to be found in aircraft, although they were found in systems which the technical community today would consider to be "adaptive."

The first truly "adaptive" materials to be used for their structural properties in aerospace systems draw their roots to the 1930's when A. Ölander discovered the pseudoelastic behavior of Gold-Cadmium alloys in 1932.[4] Six years later, Greinger and Mooradian observed the formation and disappearance of a Martensitic phase by decreasing or increasing the temperature of a Copper-Zinc alloy. The basic property of the now ubiquitous "memory effect" was reported a decade later by Kurdjumov and Khandros and by Chang and Read.[5] Although these stoichiometries of SMA's were interesting, they did not hold much promise as significant strain levels were not readily produceable, their power consumption was extremely high with respect to other adaptive materials, response was slow and machining techniques were challenging at best. Between 1962 and '63, one of the most significant metallurgical advances was made nearly by accident at the US Naval Ordinance Laboratory. A small piece of test material was bent repeatedly in a laboratory management meeting. One of the Associate Technical Directors, Dr. David Muzzey reportedly held his pipe lighter underneath the drastically bent sample... and much to everyone's amazement, it stretched back into its original shape.[6,7]

Following this serendipitous discovery, the Nickel-Titanium line of SMA's have essentially supplanted most other stoichiometries and lead to a number of important aerospace product lines. Perhaps foremost among them is the line of SMA hydraulic line couplers initially produced by Raychem Corporation. Their Cryofit™ line of tube couplers were first introduced in 1969. These "shrink-to-fit" tube couplers solved the problem of coupling hydraulic fluid lines on the Grumman Aerospace Corporation F-14.

Fig. 1 Grumman F-14D Tomcat -- the First Aircraft Fielded with Man-Made Adaptive Materials

Grumman engineers were seeking new technologies to solve the difficult task of joining lines that lie close to the aircraft's aluminum skin. Raychem Corp., which had wide experience in heat-shrinkable plastics, proposed a coupling in which a low- Temperature Transition Range (TTR) (below –120 °C; –184 °F) Nitinol alloy was fabricated at room temperature (in the Austenite phase) to the final *deployed* coupling dimensions which were just slightly below the coupling tube's outer diameter. To produce the desired coupling effect the coupler was placed in a liquid nitrogen bath so as to cool the SMA and generate a Martensite phase throughout the alloy. Given this low range of A_s, A_f, M_s and M_f, all transitions would be complete during normal aircraft operation. While in the nitrogen bath, the coupler was radially expanded. This was accomplished by forcing an oversized tapered plug through the coupler bore. When continually cooled in liquid nitrogen, the coupler remained expanded. Coupling two sections of hydraulic pipe was then accomplished by simply inserting the tube ends into the cold, expanded Nitinol coupler and allowing the coupler to warm to its near original, or Austenitic diameter. The radial contraction of the coupler, combined with the very high associated force, provided a continuously clamping and totally sealed joint at well below the required –120 °C (–184 °F) temperature.[10,11] In this Nitinol application the TTR was designed to be less than –120 °C (–184 °F), which was the required minimum operating temperature specification of the aircraft at high altitude.

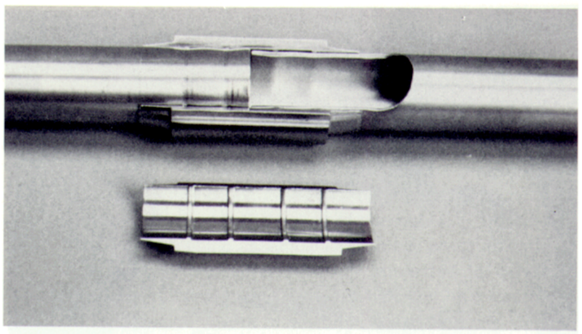

Fig. 2 Raychem Corporation Cryofit™ SMA Tube Coupler

These proven couplers are currently being used to join hydraulic tubes in the F-14 fighter aircraft as well as in many other similar applications.[11] A number of other companies also sell tube couplers with SMA in various components, but this original application by Raychem Corp. had a profound impact on the technical community as it was the first time that SMA's had appeared in front-line aircraft. Raychem continued their success with the introduction of Tinel Lock™ rings for electrical shielded cables. Fig. 3 shows how simple the installation techniques are:

Fig. 3 Raychem Corporation Tinel Lock™ SMA Cable Shielding Termination

To assemble, a technician simply assembles the components (left), screws an adapter head on (center), then heats the Tinel Lock™ ring by using electrical resistance.

Throughout the 1970's most adaptive structures technologies revolved around SMA and their many applications. The 1980's however, were quite different.

Many adaptive aerostructures projects have been conducted which did not lead to flightworthy components, but were instrumental in the overall development of the technology. Fundamental design principles, modeling techniques and much interest in the technical community were established during these programs. The earliest adaptive aerostructures leading to flight control dated from the mid 1980's and were pioneered by Ed Crawley, Steven Hall and other researchers at MIT.[12-15] These early endeavors included bending-twist coupled plates which were exposed to airloads and actively bent by piezoceramic sheets which were laminated on either face of the plates. The bending deformations induced twist, which in turn, increased airloads and bending moments, eventually leading to static aeroelastic divergence. These early endeavors also included work on the first of the piezoelectric adaptive flaps which demonstrated aerodynamically useful deflection levels on the order of several degrees. The first twist-active piezoceramically actuated missile wing and helicopter rotor blades were designed and prototyped between 1989 and 1990. These structures used the concept of directional attachment which gave otherwise isotropic actuator elements (like piezoceramic sheets) highly orthotropic properties. Given orthotropy levels in excess of 100 ($E_L > 100E_T$), these Directionally Attached Piezoelectric (DAP) sheets were oriented at off-axis angles so as induce torsional shear flows to twist structures.[16-19] Although rotor blade static twist deflections of only ±0.3° were generated (i.e. not enough for flight control) because elements were only laid from the 5 to 35% chord, the full-scale DAP cruise missile wing showed ±0.8° of deflection. These deflections produced rolling moments which were enough for full roll control equivalent to many aileron configurations. Given that the wings would continuously twist without surface gapping, this also had important implications for low observables aircraft. Extensive studies on the aeroelastic properties of forward and aft swept DAP wings were made by Weisshaar and Ehlers.[20-22] They showed among other things that DAP wing twist deflections be controllably magnified through aeroelastic coupling generated by structural tailoring and/or wing sweep.

DAP elements made their way into a twist-active supersonic missile wing and a subsonic missile fin in 1991.[23-25] The resulting Constrained Spar Torque-Plate Missile Fin effort demonstrated ±4.5° static deflections with no aeroelastic divergence problems or use of aeroelastic amplification methods. This project represented the first time an adaptive aerostructure was built with collocated elastic axis, lines of aerodynamic centers and centers of gravity. Figure 4 shows the

Constrained Spar Torque-Plate Missile Fin undergoing activation.

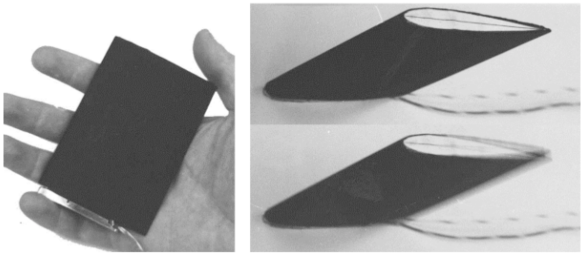

Fig. 4 DAP Fin Undergoing Excitation (1991)

Although the constrained-spar torque plate design functioned very well at lower Mach numbers, the growth of the strength of the main spar with increasing Mach number also induced a similar boost in torsional stiffness. Because the main spar and the torque-plate were mechanically joined, the total deflection levels decreased as design Mach number increased. Accordingly, it became apparent that it was necessary to decouple the torque plate from the main spar to maintain good deflection performance. The resulting free-spar torque-plate fin would produce the highest static pitch deflections at the time of ±7° while sporting a main spar sized for Mach 0.7 airloads.[26]

Following the award of one of the first adaptive missile fin contracts, a number of subsonic and supersonic missile fin concepts were studied along with basic actuator characteristics which are germane to flight control.[26] These concepts included several different section subsonic and supersonic airfoil section profiles and both twist-activation and camber control, using finite element modeling techniques. Several significant conclusions were drawn from the experiences of Ref. 26. Chief among them was the realization that low aspect ratio flight control surfaces which were designed to carry full high α, high speed flight loads could not be made to actively deform enough to achieve suitable levels of flight control, even when using 10% strain actuation levels associated with shape-memory alloys for structural materials. Rather, it was shown that gross structural rotational deflections of entire flight control surfaces were necessary to achieve forces and moments which were usable for most classes of subsonic and supersonic missiles. Figure 5 shows a 2% thick double circular arc supersonic missile fin undergoing a camber deformation beside a NACA 0012 subsonic missile fin being actively deformed in twist.

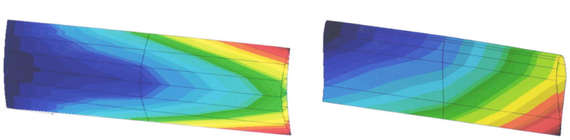

Fig. 5 DAP Fin Undergoing Camber & Twist Deflections (1993)

The first full missile configuration to be tested with an adaptive wing was centered on a modified TOW-2B. Because nearly 1/3 of the weight and volume within the TOW missile was devoted to flight control, there existed a tremendous opportunity to bring substantial benefits by packing all of the flight control systems within the missile wings themselves. The project showed that room for at least one more warhead would be opened up, range could be increased (with a larger spool), engagement time reduced and it would become so maneuverable that it could hit targets up to 135° off boresight.[27,28] The enabler behind the TOW-2B effort was the Flexspar solid state adaptive stabilator technology. Although invention disclosures were filed in the Fall of 1994 with the Auburn University Office of the Vice President for Research, no patents were ever applied for. This firmly cast the technology in the public domain and freed any future investigator from intellectual property revenue claims. This is liberating for the technical community at large as, to this day, Flexspar stabilators have been shown to generate some of the highest pitch deflections of any known arrangement of internally mounted adaptive stabilator actuators using piezoceramic actuator elements. Even without aeroelastic tailoring, deflections in excess of ±30° can be achieved by these actuators.[29] Figure 6 shows the 1/3 scale TOW-2B missile model with Flexspar wings mounted in the wind tunnel just prior to testing.

Although the Flexspar technology provided good performance to missiles, a need for bolstering close-in aerial combat capabilities was identified in the US Air Force. Because the closest aerial engagements are often conducted with cannon, a program to lend guidance to air-to-air cannon shells was spawned. This marked the first time that adaptive aerostructures would be designed into munitions which would be hard-launched with setback accelerations of up to 40,000g's. The Barrel-Launched Adaptive Munition (BLAM) program was active from 1995 through 1997 and showed that a conically shaped hard-launched munition could be built to maneuver by pitching the nose section about a ball joint in the nose which was collocated at both the aerodynamic center and the center of gravity.[30-33] Figure 6 shows the prototype BLAM round mounted in the supersonic wind tunnel. Although the BLAM program represented the first time an adaptive aerostructure had been tested supersonically, perhaps the most important contribution to the field of adaptive aerostructures was through the establishment of manufacturing principles for piezoceramic actuator hardening.

At the same time that the BLAM program was underway, the Smart Compressed Reversed Adaptive Munition (SCRAM) effort was starting. Like the BLAM, it too was a munitions effort, but with a distinctly different set of design criteria. As a softlaunched area weapon, its overarching design specifications spoke to GPS guidance and maximum volumetric compression. This volumetric compression was critical to allow aircraft like the F-22 achieve respectable loadouts with weapons larger than 250lb. Because antagonistically configured piezoceramic sheets could be convienently arranged within body strakes, the robust actuators were fully capable of driving the switchblade fins a full ±10° in pitch deflection at rates in excess of 50 Hz through the entire transonic flight regime.[34,35] Again, more new territory was being charted as this was the first adaptive aerostructure to demonstrate full utility through this Mach range which is notorious for challenging actuators with its centers of pressure shifts and resulting large control moments. Figure 6 shows the SCRAM mounted in the wind tunnel prior to testing.

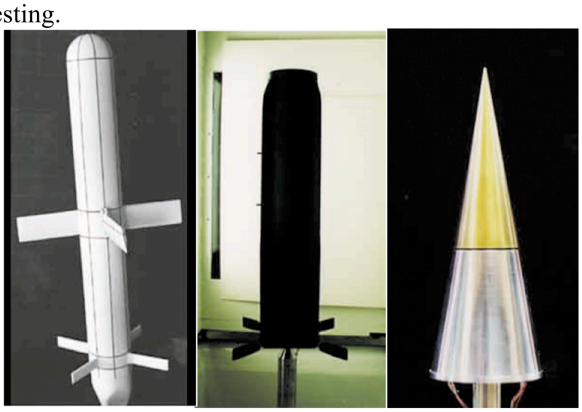

Fig. 6 Adaptive TOW-2B, SCRAM and BLAM Models Mounted in Various Wind Tunnels

Although area weapons were and are of great interest to the US Air Force, penetrators were becoming increasingly important. To meet the demands of weapon compression, several families of 250 lb penetrators of the Miniature Munition Technology (MMT) configuration have been designed for internal carriage. To aid in terminal guidance a canard kit using internally mounted piezoceramic actuators was designed using the Rotationally Active Linear Actuator (RALA) configuration for the US Air Force's WIDT program. Because no volume outside of the aerodynamic shells could be used to house actuators (to maintain the integrity and form factor of the penetrator head), all actuator materials were forced into the aerodynamic shell. To maintain high moment generation capability, an actuator which was capable of generating high torque levels was used. Given a constrained volume and high moment requirements, the resulting deflections were on the order of only ±2°, which is suitable for vernier control in the terminal phase.

In 1998 Flexspar technology was applied to a different flight regime. This time, instead of being used for low speed missiles and UAVs, it was integrated into Mach 3+ projectiles in the Range-Extended Adaptive Munition (REAM) program. This project would advance the field of piezoelectric actuation further by extending it to control of aerodynamic surfaces in supersonic flow around a hard-launched munition.[38,39] Bench and wind tunnel tests confirmed its utility in the mid supersonic flight range. Although other investigators actively worked on several different incarnations of adaptive fins, wings and canards, designers experienced limited deflections and therefore limited performance.[40]

The 1990's also saw the advent of advanced adaptive rotorcraft concepts. The first rotary-wing aircraft to take flight used an adaptive rotor driven by DAP elements.[41-43] These were expanded to the first Micro Aerial Vehicles (MAVs) which first flew in September, 1997 and used piezoelectric elements for all flight control.[44-45] Fixed-wing aircraft were also made using SMA's for flight control[46] and the MAVs were evaluated in extremely harsh flight environments including extreme gusts and monsoon rains.[47] The ultimate need for adaptive aerostructures actuators came during the development of the XQ-138 convertible UAV. This remarkable aircraft has the capability of hovering like a helicopter, then popping up and transitioning to missile-mode flight. It was initially laid out such that it could accommodate either conventional or adaptive actuators.[49] However good the state of the art in conventional electromechanical actuators, an expansion in useful load and actuator bandwidth was needed, so a new branch of advanced adaptive actuators was born.

Advanced Adaptive Actuator Modeling

In the late 1990's a new approach to adaptive structures was conceived. Up until that time, all investigators, including this author used linear piezoelectric and/or SMA actuators. These actuators would generate a deflection in response to an applied field or current flow which was such that the greater the deflection, the lower the blocked force resistance capability. This clearly worked fine for certain missiles, munitions and UAVs like the MAVs, but as with all aerospace systems, the ever-present push for lower weight, volume, higher bandwidth and control authority necessitated a different approach. Fortunately, in 1997 Lesieutre et al came up with just such a breakthrough.

The approach taken by Lesieutre was to essentially null much of the passive stiffness of the actuator element, thereby allowing much larger deflections. These LNPS and ZNPS structures clearly showed dramatic performance improvements. Although his team used this approach only to improve the performance of electrical transformers, the concept had been successfully demonstrated.[49,50] To the adaptive structures community, this was extremely important as it was the first time that an adaptive structure exhibited an electrical-to-mechanical conversion efficiency close to 1.

To take advantage of the principles laid out in Ref.'s 49 and 50, a piezoelectric bender element is arranged in a pin-pin configuration with an externally applied axial force which is close to the perfect column buckling load. The axial force, F_a, is applied so that as the piezoelectric moment is applied, a controlled "imperfection" induces further, but controlled deformation. The overall goal of this Post-Buckled Precompressed (PBP) actuator assembly is to simultaneously and controllably amplify both the force and deflection levels which can be generated by solid state piezoelectric bender elements. The addition of various forms of compliant mechanisms on either end of the actuator allow for a higher level of controllability, but generally retard the ultimate deflection levels so the size, weight and complexity of such mechanisms are typically minimized. Because essentially any level of deflection can be excited via the application of ever higher loads, great care is taken in the design as the external face of the convex actuator element will suffer from various forms of tensile failure including depoling and mechanical fracture if the bending levels are too high. Figure 7 shows the overall arrangement of the actuator including the pin-pin supports, axial force and generic end extensions.

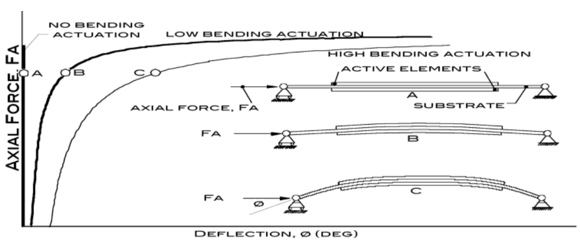

Fig. 7 Basic Post-Buckled Precompressed (PBP) Actuator Concept

The static behavior of the unloaded PBP bender element is easily captured by using classical laminated plate theory (CLPT) models. The bender is made from two primary components: a pair of piezoelectric actuator sheets bonded to a structurally stiff substrate. As the piezoelectric sheets are commanded to alternatively expand and contract, the bender element deflects up and down. An important aspect of the design involves the use of coefficient of thermal expansion (CTE) mismatch which has been used for more than 20 years to precompress tension-sensitive piezoceramic elements and pretension usually metallic isotropic substrates.[52-55] The static, unloaded (F_a= 0) behavior of the device can be modeled easily by the techniques described in Ref. 56 and 14. Assuming an unloaded structure and using CLPT methods, the following holds. The applied forces and moments may be balanced by stress distributions which are distributed through the thickness of the element:

$$N = \int \sigma dz \qquad M = \int \sigma z dz \tag{1}$$

Actuator in-plane forces and moments (a) can be expressed as a balance with external forces and moments (ex) and forces and moments due to mismatches in coefficients of thermal expansion (t). These factors will generate in-plane laminate strains, ε and curvatures, κ.

$$\begin{Bmatrix} N \\ M \end{Bmatrix}_{ex} + \begin{Bmatrix} N \\ M \end{Bmatrix}_{a} + \begin{Bmatrix} N \\ M \end{Bmatrix}_{t} = \begin{bmatrix} A & B \\ B & D \end{bmatrix}_{l} \begin{Bmatrix} \varepsilon \\ \kappa \end{Bmatrix} \tag{2}$$

If the external forces and moments are ignored and thermally induced stresses are not considered, equation 2 can be reduced to:

$$\begin{bmatrix} A & B \\ B & D \end{bmatrix}_{l} \begin{Bmatrix} \varepsilon \\ \kappa \end{Bmatrix} = \begin{bmatrix} A & B \\ B & D \end{bmatrix}_{a} \begin{Bmatrix} \Lambda \\ 0 \end{Bmatrix} \tag{3}$$

At this point, equation 3 can be easily solved for laminate curvature, κ, by assuming that a balanced, symmetric laminate composed of isotropic or quasi-isotropic elements are used:

$$\kappa = \frac{B_a}{D_l}\Lambda \tag{4}$$

By using the unloaded laminate curvature, κ, as a starting point, the problem can now be defined in terms of gross curvatures with externally applied axial force, F_a, as follows:

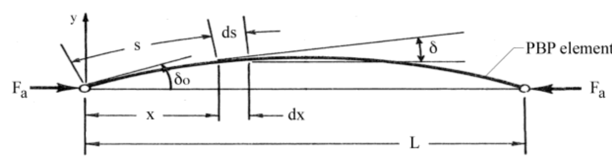

Fig. 8 Basic Nomenclature and Conventions for Analyzing a PBP Beam

Figure 8 shows that the length along the surface of the element, s, and the length along the major axis of the element, x, are related by the curvature induced in the actuator. The angular coordinate, δ is maximized at the ends of the element, δ_o and goes to zero at the mid point.

One can consider the normal strain of any point in the PBP actuator at a distance y from the neutral axis through its thickness as:

$$\varepsilon = \frac{y d\delta}{ds} = \frac{\sigma}{E} \tag{5}$$

If one examines the individual beam element and assumes pure bending, then the following holds:

$$\sigma = \frac{My}{I} \tag{6}$$

Accordingly, combining equations 5 and 6 with CLPT conventions and terminology, equation 7 is obtained:

$$\frac{y d\delta}{ds} = \frac{My}{Db} \tag{7}$$

Because the externally applied moment loading in each section comes from the axial force, F_a:

$$M = -F_a y \tag{8}$$

Substituting equation 8 into 7 yields:

$$\frac{d\delta}{ds} = -\frac{F_a y}{Db} \qquad (9)$$

Differentiating equation 9 with respect to s:

$$\frac{d^2\delta}{ds^2} = -\frac{F_a}{Db} Sin\delta \qquad (10)$$

Multiplying through by the integrating factor $2 d\delta/ds$:

$$2\frac{d\delta}{ds}\frac{d^2\delta}{ds^2} = -2\frac{F_a}{Db} Sin\delta \frac{d\delta}{ds} \qquad (11)$$

Integrating equation 11 yields:

$$\left(\frac{d\delta}{ds}\right)^2 = 2\frac{F_a}{Db} Cos\delta + a \qquad (12)$$

If one considers the addition of an applied moment via piezoelectric elements as generating an imperfection across the beam, then the unknown integrating factor, a, can be solved for, given that at x=0, $\delta = \delta_o$, $d\delta/ds = \kappa$.

$$\left(\frac{d\delta}{ds}\right)^2 = 2\frac{F_a}{Db}\left(Cos\delta - Cos\delta_o\right) + \kappa^2 \qquad (13)$$

With appropriate trigonometric substitutions and considering the negative root because dδ is always negative:

$$\frac{d\delta}{ds} = -2\sqrt{\frac{F_a}{Db}}\sqrt{Sin^2\left(\delta_o/2\right) - Sin^2\left(\delta/2\right) + \frac{\kappa^2 Db}{4F_a}} \qquad (14)$$

For solution, a change of variable is as follows:

$$Sin\left(\delta/2\right) = cSin\xi \qquad (15)$$

Where ξ is a variable with the value π/2 when x = 0 and the value 0 when x = L/2. Accordingly, when x = 0:

$$c = Sin\left(\delta_o/2\right) \qquad (16)$$

Solving for δ and differentiating yields:

$$\delta = 2Sin^{-1}\left(Sin\left(\delta_o/2\right)Sin\xi\right) \qquad d\delta = \frac{2Sin\left(\delta_o/2\right)Cos\xi}{\sqrt{1 - Sin^2\left(\delta_o/2\right)Sin^2\xi}}d\xi \qquad (17)$$

Combining eqns. 14 -17 with appropriate end values:

$$\sqrt{\frac{F_a}{Db}}\int_0^{L/2} ds = \frac{L}{2}\sqrt{\frac{F_a}{Db}} =$$

$$\int_0^{\pi/2} \frac{Sin\left(\delta_o/2\right)Cos\xi}{\left(\sqrt{Sin^2\left(\delta_o/2\right)Cos^2\xi + \frac{\kappa^2 DB}{4F_a}}\right)\left(\sqrt{1 - Sin^2\left(\delta_o/2\right)Sin^2\xi}\right)}d\xi \qquad (18)$$

Advanced Adaptive Actuator Intellectual Property Claims and State-of-the-Art Applications

Because the innovations enabled by PBP actuators are so profound, steps were taken more than 5 years ago to protect the intellectual property as relates to aerospace systems. Fig. 9 shows the basic structure of the PBP actuator element with both internally generated and externally applied axial force elements (20, 40, 50), mounting pins (30) and active elements (10). As the elemental imperfection is increased via the energization of the active element, the curvature increases. This curvature increase is helped along by the multiple axial compression members.

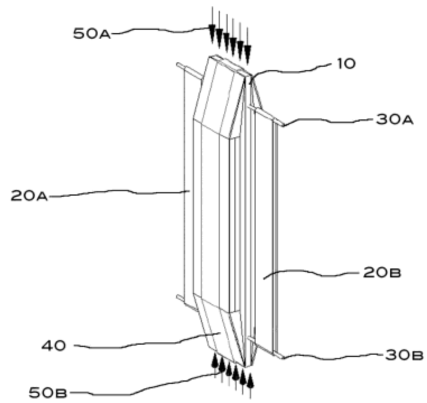

Fig. 9 Basic PBP Element[52]

This basic arrangement of active element has now been used many times over. Starting in 2004, PBP actuators have been used to control morphing aircraft[53] and have even made their way into ultra-high performance post-stall maneuvering, convertible UAVs. Figure 10 shows the XQ-138 taking off from an armored vehicle at Redstone Arsenal, Alabama.

Fig. 10 XQ-138 PBP-Controlled High Performance Convertible UAV Launching, Transitioning and Flying Out from an Armored Vehicle at Redstone Arsenal, AL

In addition to enhancing some of the world's high performing UAVs, PBP technology is revolutionizing the world of flight flutter testing. Figure 11 below shows the internal structure of one of the most advanced flight flutter test surfaces in the world.

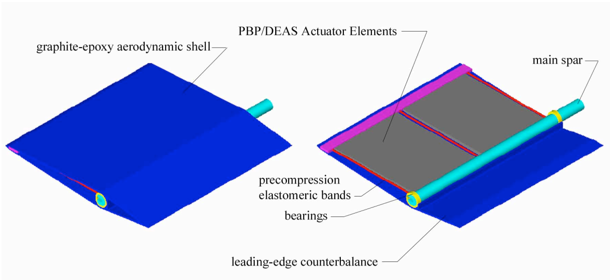

Fig. 11 PBP-Driven Transonic Flutter Test Surface

The PBP flutter test surface using Dynamic Elastic Axis Shifting (DEAS) is currently undergoing development and demonstration at SkyShaker Technologies (SST) LLC of Lawrence, Kansas. Unlike conventional DEI flutter test vanes which are used today, the SST vane weighs an order of magnitude less, has much higher bandwidth, and most importantly, its exact position in space and time can be controlled to within 11ms. This means that unlike the DEI vane, the SST vane can be actuated in or out of phase with respect to other vanes on the aircraft. This is most useful for excitation of symmetric and/or antisymmetric flutter modes. Currently this type of flight test capability does not exist with conventional electromechanical actuators because they are too slow and consume too much high current power, which drives up the weight of actuator cables. The SST vane does not possess any of these challenges and is therefore poised to significantly help the entire field of flight flutter testing. Figure 12 shows the test vane prior to installation on an aircraft.

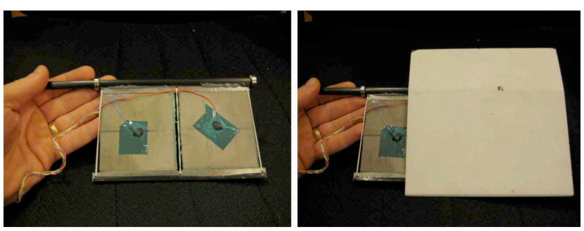

Fig. 12 SkyShaker Technologies, LLC Flutter Test Vane PBP Actuator Core and Assembly

Of course, the reason why PBP technology is used on the SST vane is because it significantly outperforms conventional electromagnetic and adaptive actuators by a significant margin. Figure 13 shows the deflection increases as a function of axial applied force levels:

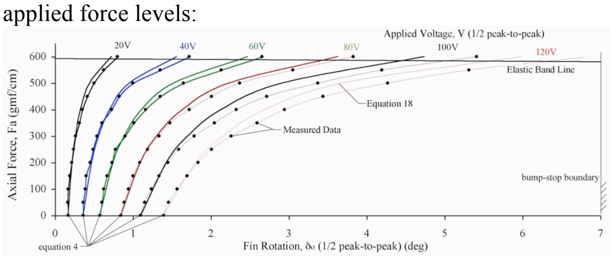

Fig. 13 SkyShaker Technologies Flutter Test Fin Rotation Amplification via the PBP Effect

From Fig. 13 it can be seen that amplification ratios, AR, on the order of 4 to 5 are achieved by using PBP techniques. This means that a conventional adaptive actuator structure will either weigh 4-5 times more to produce the same performance, will be 4-5 times the volume and/or will cost 4-5 times as much. Clearly, the 3.6% weight penalty and 15% IP license fee is more than worth an order of magnitude greater performance.

In addition to high performance flutter test vanes and UAVs, the SST, LLC is also using PBP IP in guided missiles, munitions and their Steerable Adaptive Bullet (StAB) program. Fig. 14 shows one of the few unclassified, unlimited distribution figures relating to this technology as it is employed in missiles, munitions, guided cannon shells and bullets.

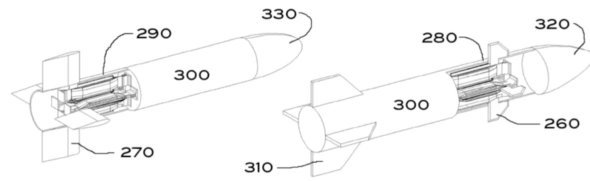

Fig. 14 PBP FCS Systems for Missiles, Munitions, Guided Cannon Shells and Bullets[52]

Optically Adaptive Materials: Leading the Way to Visual Stealth

The idea of visual stealth has been thought of for countless thousands of years. From the Helmet of Invisibility of the Greek God of the Underworld, Hades, forward, the idea of being invisible has been appealing. This has certainly proven to be the case with aircraft. Most efforts to date on aircraft have been centered on acoustic and radio frequency stealth. However, visual stealth is just as important and is now enabled by optically adaptive materials.

The concept of visual stealth has its roots in a 1943 U.S. Navy project codename Yehudi. The intent of the program, which was highly secret at the time and came to light only in the 1980s, was to give Navy patrol aircraft a better chance of sinking enemy submarines. As allied aircraft scrambled to attack U-boats, submarine captains called for crash dives whenever they spotted approaching attack planes. By the time an aircraft got close enough to sink a sub, it had disappeared. Yehudi's inventors needed a way to make the aircraft harder to see, and they realized that camouflage paint wouldn't do the job: Regardless of its color, the airplane would be a black dot against the sky. The engineers fitted a TBM-3D Avenger torpedo-bomber with 10 sealed-beam lights, installed along the wing's leading edges and the rim of the engine cowling. When the intensity of the lights was adjusted to match the sky, the Avenger blended into the background.[57] Tests proved that the Yehudi system lowered the visual acquisition range from 12 miles to two miles, allowing the Avenger to get within striking distance of its targets before they submerged.

In addition to matching the background via differential illumination in the visible spectrum, several inventions have been conceived which work to make the aircraft wings and fuselage match the background in the infrared spectrum. Although a worthy goal, typically the thermal signatures of the propulsors generate the largest infrared signature, rather than the skin of the aircraft. Accordingly, much more effort has been and is currently being placed on suppressing the signature of aircraft in the visible spectrum.[58,59]

Although aerospace programs often make headlines, most of those efforts are restricted. On the other hand, architectural and industrial programs operate with a high level of latitude and are actively bring pursued. These have yielded quite a number of patents and reports, but fundamentally they use similar techniques.[60-71] Although the architectural approaches work in many situations, they do not typically work with all because they have a hard time eliminating under/overmatch spots at differing angles of regard.

To skirt these undermatch problems, modern methods of visual stealth have used active techniques. The overall scheme is to measure the color and luminosity of the background, then project it on the opposite side of the aircraft. These current methods all require relatively complicated and costly treatments which require major overhauls of the aircraft for installation.

These problems were fundamentally solved several years ago when the first UAVs using visual stealth treatments took to the air. Figure 15 shows a 2m UAV with a cloaking device using optically adaptive materials turned off, then turned on.

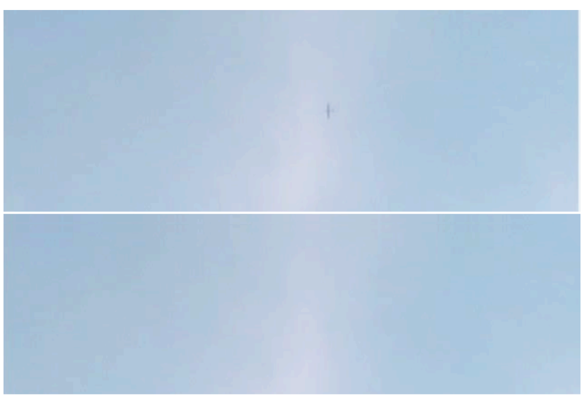

Fig. 15 Luminosity Undermatch and Match of VSS UAV Against a Cirrus Cloud Band, 300m Altitude

Clearly from Fig. 15 this technology works and works well. Space constraints prevent inclusion of further details, but suffice it to say that the aircraft becomes essentially invisible to all ground observers.

Adaptive Engine Nacelles: Improving Performance, Reducing Noise

In the late 1990's several efforts were underway to integrate adaptive structures into FAR-25 certified aircraft. Unlike smaller, uninhabited aircraft, missiles, munitions and UAVs these large commercial transports are governed by rules set forth by various regulatory agencies like the FAA. Accordingly, strict certification guidelines must be followed, which often slow the implementation of advanced technologies. Still, Boeing pressed on and showed in 2004 that significant noise reduction could be achieved during takeoff, landing and cruise by using chevrons that move to mix the jetwash as it exits the nacelle. Figure 16 sows a nacelle

Fig. 16 GE90-155B Turbofan on a Boeing 777 Fitted with SMA-Actuated Chevrons

Flight testing over an instrumented test range at Glasgow, Montana showed noise reduction levels on the order of 4db externally with more than 2db of noise reduction in the cabin.[72-75] Currently, the adaptive chevron technology is being integrated on several Boeing aircraft including the 787, 747-400QLR and the 747-8.

Summary

This paper has presented some of the most advanced adaptive structures concepts which are making significant improvements to various corners of the aerospace industry. The field was traced from its roots in the 1880's and 1930's to adaptive munitions technologies of the 1990's. The basic structural mechanics of the most advanced adaptive actuation configuration, Post-Buckled Precompressed (PBP) actuators were laid out. Fundamental structural models showed excellent correlation between theory and experiment and demonstrated an order of magnitude improvement over conventional technologies. A series of aircraft using PBP flight control devices were shown in flight including the XQ-138 convertible ultra-high performance UAV. A PBP flutter test vane and unclassified, unlimited distribution munitions designs using PBP actuators were also shown. The fundamentals of visual stealth using adaptive materials were shown along with an adaptive engine nacelle being fielded by Boeing Aircraft Corporation which generated a 4db reduction in external acoustic signature.

References

1. Taylor, G. W. et al, *Piezoelectricity*, Gordon and Breach Science Publishers, Newark, NJ, 1985.
2. Mason, W. P., *Piezoelectricity, Its History and Applications,"* Journal of Acoustical Society of America, Vol. 70, No. 6, 1981.
3. Cady, W. G., *Piezoelectricity*, McGraw-Hill, New York, NY 1946; reprinted by Dover Press, 1964.
4. Ölander, A., "An Electromechanical Investigation of Solid Cadmium-Gold Alloys, "*Journal of the American Chemical Society*, 154, 1932, pp. 3819-33.
5. Otsuka, K. and Wayman, C.M., *Shape Memory Materials*, Cambridge University Press, Cambridge, UK, 1998.
6. Kauffman, G., and Mayo, I., "Memory Metal," *Chemical Matters*, Vol. 4, No. 7, October, 1993.
7. Buehler, W. J., "NITINOL Re-Examination," WOL Oral History Supplement, WOLAAF LEAF, Vol. 8, No. I, Winter, 2006.
8. Kauffman, G. B., and Mayo, I., "The Story of Nitinol: The Serendipitous Discovery of the Memory Metal and Its Applications," *The Chemical Educator,* Springer-Verlag New York, NY, Vol. 2, no. 2, 1996.
9. D. Stockel, The martensitic Transformation in Science and Technology, ed., E. Hornbogen and N. Jost, Informationsgesellschaft-Verlag, p.223, 1989.
10. L.McD. Schetky, *Proceedings, SMST-94,* Pacific Grove, California, p.239, 1994.
11. Liu, X.; Stice, J. D. *J. of Appl. Manufacturing Systems,* Vol. 3, No. 65, 1990.
12. Crawley, E., Lazarus, K. and Warkentin, D., "Embedded Actuation and Processing in Intelligent Materials," presented at the *2nd international Workshop on Composite Materials and Structures for Rotorcraft,* Troy, NY, Sept., 1989.
13. Lazarus, K., and Crawley, E., "Multivariable Active Lifting Surface Control using Strain Actuation: Analytical and Experimental Results," paper presented at the *Third International Conference on Adaptive Structures,* sponsored by the ASME, 9 - 11 November, 1992, San Diego.
14. Lazarus, K. B., Crawley, E. F., and Bohlmann, J. D., "Static Aeroelastic Control Using Strain Actuated Adaptive Structures," Proceedings of the *First Joint U.S./Japan Conference on Adaptive Structures,* Maui, Hawaii, October, 1990.
15. Spangler, R. L., and Hall, S. R., "Piezoelectric Actuators for Helicopter Rotor Control," *31st Structures, Structural Dynamics and Materials Conference,* Long Beach, Ca, April, 1990.
16. Barrett, R., "Intelligent Rotor Blade Actuation through Directionally Attached Piezoelectric Crystals," 46th AHS National Conference and Forum, Washington, D.C., May, 1990.
17. Barrett, R., "Intelligent Rotor Blade and Structures Development using Piezoelectric Crystals," MS Thesis, the UM, College Park, Maryland 1990.
18. Barrett, R., "Method and Apparatus for Sensing and Actuating in a Desired Direction," US Pat. 5,440,193, Aug. 1995.
19. Barrett, R., "Actuation Strain Decoupling Through Enhanced Directional Attachment in Plates and Aerodynamic Surfaces," proceedings of the First European Conference on Smart Structures and Materials, Glasgow, Scotland, 12 - 14 May 1992, IOP Publishing, Bristol, UK 1992, pp. 383 - 386.
20. Ehlers, S. M., and Weisshaar, T. A., "Static Aeroelastic Behavior of an Adaptive Laminated Piezoelectric Composite Wing," AIAA-90-1078-CP, April, 1990, pp. 1611-1623.
21. Ehlers, S. M., and Weisshaar, T., "Adaptive Wing Flexural Axis Control," paper presented at the *Third International Conference on Adaptive Structures,* ASME, 9 - 11 Nov., 1992, San Diego.
22. Ehlers, S. M., and Weisshaar, T. A., "Effect of Material Properties on Static Aeroelastic Control," paper presented at the 33rd Structures, Structural Dynamics and Materials, Dallas, TX, 15 April, 1992.
23. Barrett, R., "Active Plate and Missile Wing Development Using EDAP Elements," *Journal of Smart Materials and Structures,* Institute of Physics Publishing, Ltd., Techno House, Bristol, UK, Vol. 1, No. 3, pp. 214226, ISSN 096.
24. Barrett, R., "Active Plate and Missile Wing Development Using DAP Elements," AIAA *Journal,* March, 1994.
25. Barrett, R., "Active Composite Torque-Plate Fins for Subsonic Missiles," paper presented at the Dynamic Response of Composite Structures Conference, New Orleans, Louisiana, August 30 - September 1, 1993.
26. Barrett, R., "Advanced Low-Cost Smart Missile Fin Technology Evaluation," Report to the USAF Armament Directorate, Eglin Air Force Base, FL, Contract No. F0 8630-93-C-0039, BAT, Nov 1993.
27. Barrett, R., Brozoski, F., and Gross, R. S., "Design and Testing of a Subsonic All-Moving Adaptive Flight Control Surface," *AIAA Journal*, Reston, VA,Volume 35, No. 7, July 1997, pp. 1217 - 1219.

28. Barrett, R. and Brozoski, F., "Missile Flight Control using Active Flexspar Actuators*," Journal of Smart Materials and Structures*, Institute of Physics Publishing, Ltd., Techno House, Bristol, UK, Vol. 5, No. 2, March 1996, pp. 121-128.

29. Barrett, R., "Active Aeroelastic Tailoring of an Adaptive Flexspar Stabilator," *Journal of Smart Materials and Structures*, Vol. 5, No. 6 Dec. 1996, Techno House, Bristol, UK, 1996, pp. 723 – 730.

30. Barrett, R., "Invention and Evaluation of the Barrel - Launched Adaptive Munition (BLAM)," final report for USAF contract no. F-49620-93-C-0063, USAF Wright Laboratory Flight Vehicles Branch, WL/MNAV August, 1995.

31. Barrett, R., and Stutts, J. "Barrel-Launched Adaptive Munition BLAM Experimental Round Research," final report for USAF contract no. F-49620-C-0063, USAF Wright Laboratory Flight Vehicles Branch, WL/MNAV February, 1997.

32. Winchenbach, G., "Cone Aerodynamics Test", Aeroballistic Research Facility Ballistic Spark Range Technical Report, USAF Wright Laboratory Flight Vehicles Branch, WL/MNAV June 1996.

33. Barrett, R. and Stutts, J., "Modeling, Design and Testing of a Barrel-Launched Adaptive Munition," proceedings of the 4th Annual SPIE Symposium on Smart Structures and Materials, San Diego, CA, 3-6 March 1997.

34. SCRAM Report Barrett, R., "Design, Construction and Testing of a Proof-of-Concept Smart Compressed Reversed Adaptive Munition," Final Report to the USAF Armament Directorate, Wright Laboratory, Eglin AFB, FL, AF-FO8630-95-K-0079, Sept. 1996.

35. Barrett, R., and Stutts, J., "Development of a Piezoceramic Flight Control Surface Actuator for Highly Compressed Munitions," 39th Structures, Structural Dynamics and Materials Conference 20 - 23 April 1998, Long Beach, CA, no. AIAA-98-2034.

36. Barrett, R., "Construction and Test Report for the Rotationally Active Linear Actuator (RALA) Adaptive Canard, Final Report for McDonnell Douglas, St. Louis, MO contract no. FO 8630-95-C-0009, August, 1997.

37. Knowles, G., R. Barrett and M. Valentino, "Self-Contained High Authority Control of Miniature Flight Control Systems for Area Dominance," SPIE 11th International Symposium on Smart Structures and Materials, San Diego, CA, Mar. 2004.

38. Lee, Gary, "Range-Extended Adaptive Munition (REAM)" Final Report from Lutronix Corporation to the DARPA, Del Mar, California, April 1999.

39. Lee, Gary, "40/50 Caliber Range-Extended Adaptive Munition (REAM)" Final Report from Lutronix Corporation to the US Army TACOM-ARDEC Del Mar, California, May 2000.

40. Rabinovitch, O., and J. R., Vinson, "On the Design of Piezoelectric Smart Fins for Flight Vehicles," Journal of Smart Materials and Structures," IOP Publishing, Ltd., Techno House, Bristol, UK, Vol. 12, No. 5, pp. 686 – 695, Oct., 1993.

41. Barrett, R., "High Bandwidth Electric Rotor Blade Actuator Study," Phase I SBIR proposal Submitted to the U.S. Army Aviation Systems Command, St. Louis, MO 27 June 1992.

42. Barrett, R. and Stutts, J., "Design and Testing of a 1/12th Scale Solid State Adaptive Rotor," *Journal of Smart Materials and Structures,* Vol. 6, No. 4 Aug. 1997, Techno House, Bristol, UK, 1997, pp. 491 - 497.

43. Barrett, R., Frye, P., and Schliesman, M., "Design, Construction and Characterization of a Flightworthy Piezoelectric Solid State Adaptive Rotor," *Journal of Smart Materials and Structures* Vol. 7, No. 3, June 1998, pp. 422–431.

44. Lee, G., "Design and Testing of the Kolibri Vertical Take-Off and Landing Micro Aerial Vehicle," final report for the Department of Defense CounterDrug Technology Office, November 1997.

45. Barrett, R., and Howard, N., "Adaptive Aerostructures for Subscale Aircraft," refereed proceedings of the 20th Southeastern Conference on Theoretical and Applied Mechanics," Pine Mountain, GA, 17 April 2000.

46. Barrett, R., Burger, C. and Melián J.P., "Recent Advances in Uninhabited Aerial Vehicle (UAV) Flight Control with Adaptive Aerostructures," 4th European Demonstrators Conference, 10 – 15 Dec. 2001, Edinburgh, Scotland.

47. Barrett, R. and Lee, G., "Design Criteria, Aircraft Design, Fabrication and Testing of Sub-Canopy and Urban Micro-Aerial Vehicles," AIAA/AHS International Powered Lift Conference, Alexandria, Virginia, Nov. 2000.

48. Barrett, R., "Convertible Vertical Take-Off and Landing Miniature Aerial Vehicle," US patent 6,502,787, 22 Feb. 2002.

49. Lesieutre, G.A., and C.L. Davis, "Can a Coupling Coefficient of a Piezoelectric Actuator be Higher Than Those of Its Active Material?," Journal of Intelligent Materials Systems and Structures, Vol. 8, 1997, pp. 859-867.

50. Lesieutre, G. A. and Davis, C. L., “Transfer Having a Coupling Coefficient Higher than its Active Material,” US Pat. 6,236,143 issued 22 May 2001.

51. Barrett, R. and P. Tiso, “PBP Adaptive Actuator Device and Embodiments,” International Patent Application number PCT/NL2005/000054, via TU Delft, 18 February 2005.

52. Barrett, R., Vos, R., Tiso, P. and De Breuker, R., "Post-Buckled Precompressed (PBP) Actuators: Enhancing VTOL Autonomous High Speed MAVs," Proceedings of the 46th AIAA/ASME/ASCE/AHS/ASC Structures, Structural Dynamics and Materials Conference , Austin, Texas, Apr. 18-21, 2005, AIAA paper no. AIAA-2005-2113.

53. Vos, R., De Breuker, R., Barrett, R. and Tiso, P., " Morphing Wing Flight Control Via Post-Buckled Precompressed Piezoelectric Actuators," AIAA Journal of Aircraft, Vol. 44, No. 4, pp. 1060 - 1068 July - August 2007.

54. Barrett, R., McMurtry, R., Vos, R.., Tiso, P. and De Breuker, R., "Post-Buckled Precompressed Piezoelectric Flight Control Actuator Design, Development and Demonstration," Journal of Smart Materials and Structures, Volume 15, No. 5, pp. 1323 - 1331 October 2006.

55. De Breuker, R., Vos, R., Barrett, R. and Tiso, P., "Nonlinear Semi-Analytical Modeling of Post-Buckled Precompressed (PBP) Piezoelectric Actuators for UAV Flight Control," Proceedings of the 47th AIAA/ASME/ASCE/AHS/ASC Structures, Structural Dynamics, and Materials Conference 14th AIAA/ASME/AHS Adaptive Structures Conference 7th, Newport, RI, May 1-4, 2006 AIAA-2006-1795.

56. Jones, R. M., "Micromechanical Behavior of a Lamina," *Mechanics of Composite Materials*, Hemisphere Publishing Corporation, NY, NY, 1975.

57. Anon., "Yehudi Lights," http://en.wikipedia.org/wiki/Yehudi_lights, January 2009.

58. Sweetman, W. and Douglass, S., “Hiding in Plane Sight - Stealth Aircraft Own the Night, Now They Own the Day,” Popular Science, May 1997, 54-59.

59. Sweetman, W., “The Invisible Men,” Air & Space Magazine, May 1997, pgs. 18-27.

60. Heiniger, F., “Camouflage Structure,” US Pat. 6,605,340 issued 12 August 2003.

61. Rothgeb, S. B., Bacon, K. S., and Swiney, R. L. Jr., “Structure for Concealing Telecommunication Antennas,” US Pat. Application, 10/622,840, published 29 April 2004.

62. Anitole, G., “Building Shape Modification Camouflage Structures,” US Pat. 6,257,262, issued 10 July 2001.

63. Spanier, J. and Spanier, F., “Method and Assembly for Camouflaging at Least one Building,” US Pat. 4,294,308 13 October 1981.

64. Schlenker, W. E., “On-Board Camouflage Lighting System using Directional Light Sources,” US Pat. 6,459,076 issued 1 October 2002.

65. Reynolds, R. F. and Kinsella, M. J., “Thermal and Visual Camouflage System,” US Pat. 6,338,292 issued 15 January 2002.

66. Conway, T. G., McClean, R-L G. and Walker, G. W.,” Three Color Infrared Camouflage System, “Three Color Infrared Camouflage System,” US Pat. 5,077,101 31 December 1991.

67. Grippin, R. R., “Fiber Optic Camouflage,” US Pat. 5,220,631 issued 15 June 1993.

68. Bettinger, D. S., “Orthogonal Projection Concealment Apparatus,” US Pat. 6,333,726 issued 25 December 2001.

69. Larue, J. L., “Camouflaged Structure and method of Camouflaging a Structure against a Background Having a Generally Uniform Composition,” US Pat. Application 10/726,205 1 December 2003.

70. Schowengerdt, R. N., “Cloaking System using Optoelectronically Controlled Camouflage,” US Pat. 5,307,162 issued 26 April 1994.

71. Alden, R. M., “Multi-Perspective Background Simulation Cloaking Process and Apparatus,” US Pat. Application, 09/970,368 11 July 2002.

72. Conservative, P., "Boeing Makes "Quiet" Advances (Noise-Reduction Efforts Pay Off at Remote Airfield in Montana), Seattle Post-Intelligencer, Thursday, 11 August 2005.

73. Cabell, R. H., Schiller, J.H, Mabe, Ruggeri, R.T. and Butler, G.W., "Feedback Control of a Morphing Chevron for Takeoff and Cruise Noise Reduction," ACTIVE 04, Williamsburg, VA 20-22 Sept. 2004.

74. Calkins, F.T. and Butler, B., "Subsonic Jet Noise Reduction Variable Geometry Chevron," 42nd AIAA Aerospace Sciences Meeting and Exhibit, 5 - 8 January 2004, AIAA Paper AIAA-2004-190.

75. Anon., "Boeing and General Electric Validate 747-8 Quiet Technologies," Boeing Corporation Press Release, Seattle, Washington, 20 Sept. 2006.